doi:10.1017/S1431927610057533
Microsc. Microanal. 16 (Suppl 2), 2010

Three-Dimensional Resolution Limits and Image Contrast Mechanisms in Scanning Confocal Electron Microscopy

P.D. Nellist[*], P. Wang[*], G. Behan[*], A.I. Kirkland[*], A. Hashimoto[**], M. Shimojo,[***,****] K. Mitsuishi,[***,*****], M. Takeguchi[***,******], E.C. Cosgriff[*******], A.J. D'Alfonso[*******], L.J. Allen[*******] and S.D. Findlay[********].

* Department of Materials, University of Oxford, Parks Road, OX1 3PH Oxford, United Kingdom.
** International Center for Young Scientists, National Institute for Materials Science, 1-2-1 Sengen, Tsukuba 305-0047, Japan.
*** High Voltage Electron Microscopy Station, National Institute for Materials Science, 3-13 Sakura, Tsukuba 305-0003, Japan.
**** Advanced Science Research Laboratory, Saitama Institute of Technology, 1690 Fusaiji, Fukaya 369-0293, Japan.
***** Quantum Dot Research Center, National Institute for Materials Science, 3-13 Sakura, Tsukuba 305-0003, Japan.
****** Advanced Nano-characterization Center, National Institute for Materials Science, 3-13 Sakura, Tsukuba 305-0003, Japan.
******* School of Physics, University of Melbourne, Victoria 3010, Australia.
******** Institute of Engineering Innovation, The University of Tokyo, Tokyo 113-8656, Japan.

The increase in numerical aperture allowed by the correction of spherical aberration in electron lenses leads to a significant reduction of lens depth of field. In a state-of-the-art aberration-corrected transmission electron microscope (TEM), the depth of field may be a few nanometres. An opportunity therefore exists to optically section the sample to provide three-dimensional (3D) information. Whereas tilt-series tomography can be regarded as a reconstruction from slices in reciprocal space, optical sectioning records slices in real-space, and so forming a 3D object requires little, if any, data processing. In cases where only specific slices in a sample require analysis (such as buried quantum well features), then optical sectioning allows data to be recorded directly from that feature, rather than having to reconstruct a large region of sample.

Optical sectioning experiments in aberration-corrected TEM have been demonstrated using both annular dark-field (ADF) scanning TEM (STEM) methods [1,2] and by establishing a confocal geometry to form a scanning confocal electron microscope (SCEM) [3]. A comparison of these two optical configurations is shown in Fig. 1. In this presentation we will explain the resolution limits and contrast mechanisms that apply for both coherent and incoherent imaging in the STEM and SCEM configurations, using experimental data to illustrate our conclusions. We have used the Oxford-JEOL 2200 MCO instrument fitted with two aberration correctors for these experiments.

The resolution limits that apply are most usefully illustrated by considering the 3D transfer functions in reciprocal space. The forms of these transfer function have been been considered in light optics (see for example [4]) and recently revisited in the context of electron microscopy [5,6]. In addition to resolution limits, it is also important to consider image contrast mechanisms [6,7]. For example, both ADF STEM and bright-field SCEM imaging have similar resolution limits in terms of bounds

of their transfer, both having a significant missing cone in the transfer function that would be equivalent to only tilting by a few degrees in a tilt tomography experiment. Applying both these techniques to 3D imaging of supported nanoparticles shows very different results (Fig. 2). The ADF STEM image shows significant image elongation along the beam direction (as might be expected from the missing cone), with no depth sensitivity discernable. The bright-field SCEM image shows elongated contrast, but also higher resolution features localised at the nanoparticle position. Energy-filtered SCEM presents a largely incoherent mode in which there is no missing cone and shows depth localization in the data. Recently there has been interest in an annular dark-field mode of SCEM, and this will be discussed elsewhere [8].

References

[1] Borisevich, A.Y. et al., *Proc. Nat. Acad. Sci.* **103** (2006) 3044.
[2] Behan, G., et al., *Phil. Trans. Roy. Soc. Lond. A* **367** (2009) 3825.
[3] Nellist, P.D., et al., *Appl. Phys. Lett.* **89** (2006) 124105.
[4] Frieden, B.R., *J. Opt. Soc. Am.* **57** (1967) 36.
[5] Xin, H.L. and Muller, D.A., *J. Electron Microsc.* **58** (2009) 157.
[6] D'Alfonso, A.J., et al., *Ultramicroscopy* **108** (2008) 1567.
[7] Cosgriff, E.C., et al., *Ultramicroscopy* **108** (2008) 1558.
[8] Hashimoto et al., *This Volume*.
[9] This research was supported by the EPSRC and Leverhulme Trust (UK), by Grant-in-Aid for Scientific Research (JSPS), a Bilateral Joint Research Project (JSPS), Japan, and the Australian Research Council.

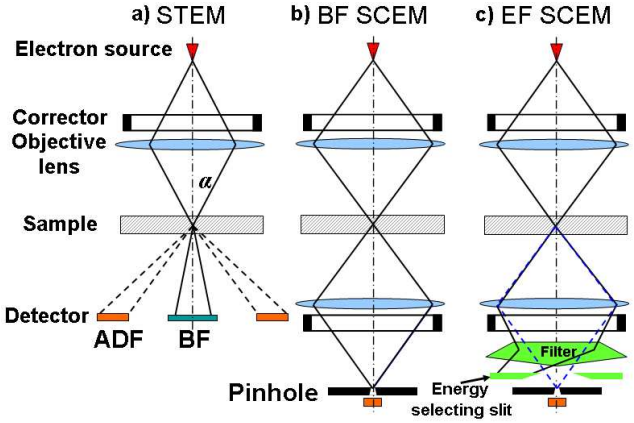

Fig 1. Schematic diagrams of the optical configurations for (a) STEM, (b) bright-field SCEM and (c) energy-filtered SCEM.

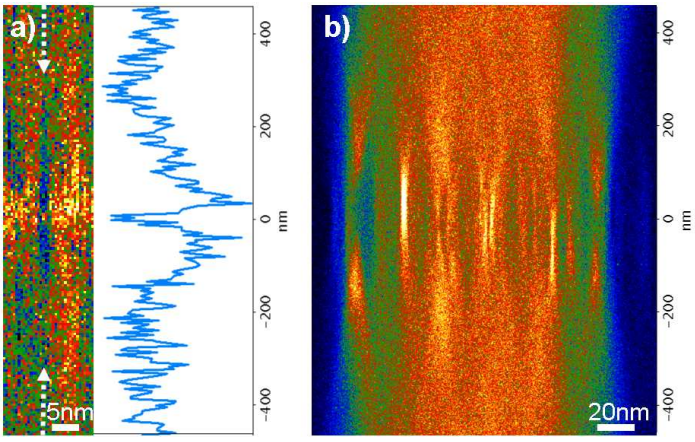

Fig 2. Projections in x-z of 3D optical sectioning data sets of supported Pt and Au nanoparticles using (a) bright-field SCEM and (b) ADF STEM optical configurations. The large elongation in the ADF STEM mode can be clearly seen. In the bright-field SCEM mode, an elongated reduction in intensity can be seen along with a more localized peak that demonstrates the transfer of high resolution information in the z direction. In (a), the profile is taken along the arrowed line.

https://doi.org/10.1017/S1431927610057533 Published online by Cambridge University Press